Available online at www.sciencedirect.com
SCIENCE DIRECT®
International Journal of Heat and Mass Transfer 47 (2004) 1367–1382
International Journal of HEAT and MASS TRANSFER
www.elsevier.com/locate/ijhmt

Modeling of 3-D non-gray gases radiation by coupling the finite volume method with weighted sum of gray gases model

D.N. Trivic *

Institute for Complex Engineered Systems, College of Engineering, Carnegie Mellon University, Pittsburgh, PA 15213, USA

Received 8 July 2003

Abstract

A new model and code for radiative heat transfer based on the numerical solution of the radiative transfer equation by finite volume method in 3-D Cartesian coordinates coupled with weighted sum of gray gases model (WSGGM) is developed. The Smith's WSGG model with 4 and 5 gray gases is used, but any other gas radiative properties model can be incorporated. The physical and mathematical concepts of the model are presented in details. The series of calculations for real gases as water vapor and a mixture of carbon dioxide, water vapor and nitrogen for uniform and non-uniform temperature fields are carried out. The predictions are compared against the rare results found in literature. The results calculated by ray tracing method with statistical narrow band model, recently published, were taken as the benchmark. The agreements with them are very good. The effects of spatial rectangular grids, of angular discretization in polar and azimuthal directions and of number of gray gases on the accuracy were analyzed. Also a new series of predictions for the mixture of 0.1 of carbon dioxide, 0.1 of water vapor and 0.8 of nitrogen on mole base is performed. It is believed that the mathematical model developed, avoiding the drawbacks of spectral lines and bands models, is sufficiently accurate and convenient for engineering calculations as well as for incorporation in computational fluid dynamics codes.

Keywords: 3-D radiation; Finite volume method; Non-gray gases

1. Introduction

Radiative heat transfer is a prevailing phenomenon in many areas, devices and equipment. That is especially the case if the temperatures are very high. These areas and devices are (i) steam generators; (ii) refinery, glass, and steel furnaces; (iii) combustion chambers of gas turbines, jet engines, and missiles; (iv) rocket nozzles; (v) solar-energy utilization; (vi) energy emission from a nuclear explosion; (vii) satellites; (viii) devices operating in space etc. There is a great necessity for mathematical models and computer codes that solve various radiation problems. The real gases as carbon dioxide, water vapor and their mixtures are mainly considered within these radiation problems. One of the important issues of the gas radiation is the description of the radiative properties of real gases or of so-called non-gray gases.

The models used for defining the radiative properties of combustion gases in radiation calculations can be roughly sorted in three groups [1]: (1) spectral line-by-line models, (2) spectral band models and (3) global models. The complexity of the models decreases from (1) to (3). Each of these models has its merits and drawbacks and consequently its area of application. Historically, the oldest and the simplest concept for the prediction of radiation in gas is gray gas model [2]. It

* Present address: Department of Thermal Engineering and Energy Research, Nuclear Institute "Vinca", P.O. Box 522, 11001 Belgrade, Serbia and Montenegro. Tel.: +381-11-245-3670x631; fax: +381-11-245-3670.

E-mail address: trivic@vin.bg.ac.yu (D.N. Trivic).

0017-9310/$ - see front matter © 2003 Elsevier Ltd. All rights reserved.
doi:10.1016/j.ijheatmasstransfer.2003.09.027

Nomenclature

a_α	absorptivity weighting factor
a_ε	emissivity weighting factor
b_ε	emissivity polynomial coefficient
c_α	absorptivity polynomial coefficient
$\hat{e}_x,\hat{e}_y,\hat{e}_z$	unit vectors in x, y, and z directions
I	radiation intensity or number of gray gas components
J	number of temperature polynomials coefficients
K	number of irradiation polynomials coefficients
$\hat{n}$	outward normal of the control volume faces
p	partial pressure
P	pressure, atm
q	heat flux
s	distance traveled by a beam
$\hat{s}$	unit direction vector
S	source function or path length, m
T	gas temperature, K
T_s	irradiation temperature, K

Greek symbols

α	total absorptivity
β	extinction coefficient
$\Delta\Omega$	control angle
ε	wall emissivity or total gas (medium) emissivity
κ	absorption coefficient
ρ	wall reflectivity
θ	polar angle measured from $\hat{e}_z$
σ	scattering coefficient or Stefan Boltzmann constant
ϕ	azimuthal (planar) angle measured from $\hat{e}_x$
Φ	scattering phase function

Superscript

l, l'	angular directions

Subscripts

b	black-body
g	gas
s	surface
i	gray gas
0	clear gas
tot	total, for all gray gases
x, y, z	Cartesian coordinate directions
α	absorptivity
ε	emissivity
λ	monochromatic or spectral values

Abbreviations

ADF	absorption distribution function
BC	boundary condition
CFD	computational fluid dynamics
CK	correlated k-distribution (method)
DOM	discrete ordinate method
DTM	discrete transfer method
EWBM	exponential wide band model
FSCK	full-spectrum correlated k-distribution (model)
FVM	finite volume method
HITRAN	high-resolution transmission absorption (database)
LBL	line-by-line (model)
RTE	radiative transfer equation
SLW	spectral line-based weighted sum of gray gases (model)
SNB	statistical narrow band (model)
3-D	three dimensional
WBM	wide band model
WSGGM	weighted sum of gray gases model
4gg	3 gray gases + 1 clear gas
5gg	4 gray gases + 1 clear gas

assumes that the gas absorption coefficient is constant within entire region of wavelengths. This model compared with others gives the predictions of very poor accuracy [3]. The line-by-line (LBL) model provides the best accuracy. In this method radiative transfer equation (RTE) is integrated over detailed molecular spectrum for the gases [4]. Because of the enormous amount of computational requirements, this model is used only for benchmark solutions.

The statistical narrow band model (SNB) is very accurate in the prediction of radiative transfer in high temperature gases. It gives the spectral transmissivity averaged over a narrow band. Because of that, it is difficult to couple SNB model to the solution method of radiative transfer equation such as finite volume method (FVM) where the values of spectral (monochromatic) absorption coefficient or its average over a wavelength interval is needed. Also the disadvantage of SNB model is that it requires a large number of bands, and therefore is very expensive for computation. Wide band model (WBM) is a simplification of the SNB model. Instead of spectral lines, it works with bands and is more economical. WBM is less, but still reasonable accurate. It yields wide band absorptance while the solution of RTE by FVM operates either with spectral or with averaged absorption coefficient. Therefore WBM cannot easily and simply be incorporated in FVM. In addition, the WBM requires the knowledge of the path length in the model as well as the spectral parameters associated with path length.

LBL, SNB and WBM are very accurate gas radiative properties models, but they require enormous amounts of computer time. This is undesirable even nowadays when powerful supercomputers are available since a gas radiative properties model is only a part of a radiation calculation. A radiation calculation is in turn only a part of a complex computational fluid dynamics (CFD) code. A CFD code that describes fire and combustion comprises 3-D turbulent multiphase fluid flow, chemical reactions and heat transfer by radiation, convection and conduction.

The correlated k-distribution method known as CK model [5,6] has been originally developed for atmospheric radiation and meteorological applications. The premise of the method is that the intensity of black-body radiation within a spectral band is constant because the band is sufficiently narrow. Also the exact position of each spectral line is not required for the computation. The intensity of radiation varies with gas absorption coefficient and in this model the absorption coefficient is reordered into a smooth function that monotonously increases. Instead of spectral integration over wavenumber inside a band, here a quadrature over the absorption coefficient was carried out. In this way the application of gas radiative properties by CK model to the solution method of RTE is much easier than for the band models like NBM and WBM. The CK model needs a vast amount of spectral data and also is very computationally expensive. In addition the CK method gives poor accuracy in the regions with extreme temperature change. This is due to presence of ''hot lines'' that were not taken into consideration. The same is with HITRAN database [1] that is an acronym for high-resolution transmission absorption database [7]. The Air Force Geophysical Laboratory has basically developed HITRAN for atmospheric radiation. It was used within spectral line-based weighted sum of gray gases model (SLW) [8]. The drawbacks of various, including the newest (1996, 1998) versions of HITRAN for high temperature gases are discussed [1]. There are several improvements of CK method in order to reduce the vast computational requirements as application of approximate methods to overlapping bands of gas mixture [9], inventions of quadrature schemes [10], using wide bands instead of narrow bands [11] and band lumping strategy by treating together the groups of narrow bands [12].

The SLW model [8,13] appeared as a more accurate version of WSGG. Within SLW the weights of classical weighted sum of gray gases model (WSGGM) were evaluated by using the absorption-line black-body distribution function. This function is calculated directly from the high-resolution molecular spectrum of gases. Instead of integration of RTE over wavenumber, now the quadrature is carried out over absorption cross section. Very similar to SLW model is the absorption distribution function (ADF) concept [14,15]. It differs from the SLW model only how the weighting factors are calculated. The weighting factors are evaluated in such a way that emission of an isothermal gas is strictly calculated for actual spectra.

Modest has shown [16] that WSGG model can be generalized for use with any arbitrary solution method of RTE. This method needs evaluation of the gray gas weighting factors and absorption coefficients (for each gray gas) for any used gas species or their mixtures.

Recently Modest and Zhang have developed a new full-spectrum correlated k-distribution model (FSCK) [1]. This concept has extended CK model over whole spectrum. The model was done by defining a fractional Plank function and by combining CK model with WSGG model. It was applied to one-dimensional problems for CO_2–N_2 mixtures showing very good accuracy. FSCK like the other CK models gave poor accuracy in cases of the extreme temperature gradients.

The global gas radiative properties models as (1) Hottel and Sarofim's [2], (2) Steward and Kocaefe's [17,18], (3) Smith et al.'s [19] are based on the concept of WSGG. The WSGG model was first established by Hottel and Sarofim [2]. It replaces the radiative properties of real gases or of non-gray gases with an equivalent finite number of gray gases. WSGG model is used for evaluation of total gas emissivity and total gas absorptivity for a given path length. For each of the gray gases, the absorption coefficient taken as no-temperature dependent, and the weighting factors taken as temperature dependent in polynomial form, should be evaluated. Even WSGG is established for the evaluation of gas emissivity and absorptivity, when WSGG is coupled with the solution of RTE only absorption coefficients and weighting factors of gray gases are used and never the total gas radiative properties.

Almost all the comparisons of various gas radiative properties models were carried out in one-dimensional geometries. There are only a few papers that report the radiative transfer from non-gray gases in 2-D and 3-D enclosures.

Maruyama and Guo [20] predicted radiative heat transfer in a 3-D boiler furnace taking prescribed temperature and concentration fields. They used the Elsasser NBM and the Edwards WBM coupled with ray emission model. Their predictions would be unacceptable expensive if a CFD code and chemical reactions were also taken into the model. The radiative transfer were calculated in 2-D, i.e. in axisymmetric cylindrical enclosures [21,22] by using statistical NBM with a ray tracing method. Besides that, in [21] was used WSGG model and in [22] the Edwards WBM. Also the statistical NBM combined with a ray tracing method was used in axisymmetric cylindrical enclosure in [23]. The predictions based on the ray tracing method are extremely expensive and cannot be used to standard engineering calculations due to difficulties related to the

linking of the RTE with NBM and WBM discussed above.

A jet flame was modeled by the coupling WBM with discrete transfer method (DTM) in [24]. The calculations of radiative heat transfer in the axisymmetric cylindrical enclosures were carried out by the SLW model and discrete ordinate method (DOM) in [25]. A very thorough comparison of various gas radiative properties models in 2-D geometries is reported in [26]. As a benchmark the statistical NBM by Malkmus was used for comparisons with WBM, CK, SLW and WSGG models. Here five 2-D enclosures were analyzed.

Trivic [27] has developed a 3-D mathematical model for predicting turbulent flow with combustion and radiative heat transfer within a furnace. The model consists of two sections: (1) Transport equations that are non-linear partial differential equations solved by a finite difference scheme and (2) the radiative heat transfer that was analyzed by the zone method. The link between these two sections is a source-sink term in the energy equation. The radiative properties of combustion gases were represented by two different models: (1) Hottel and Sarofim's model and, (2) Steward's model. The Monte Carlo method was used to evaluate total radiative interchange in the system between zones. The Mie equations were used for the determination of the radiative properties of particles suspended in the combustion gases. The mathematical model was validated against experimental data collected on two large furnaces: (1) a tangentially pulverized coal fired boiler of 220 MW; (2) an oil fired boiler of 345 MW, with symmetrically positioned burners at the front and rear wall. The tests and calculations were performed for several loads for both boilers. The measured and predicted gas temperature and heat flux distributions within the boilers were compared. The results gave reasonable agreement between measurements and values predicted by the model.

A series of calculations with varying gas radiative property models, loads, types of fuel, excess air, burner tilt angles and several particle parameters were performed [27]. The effects of these variables on the gas temperature and heat flux distributions within the furnace were studied. Steward and Trivic studied non-gray gas and particle radiation in a pulverized-coal-fired boiler [28]. A mathematical model based on the fundamental equations of motions and energy transfer, and on the zone method for determining radiative heat transfer, was developed for an operating 220 MW pulverized-coal-fired boiler. The model is capable of predicting velocity, temperature and heat flux distributions for the 3-D combustion chamber. The Steward and Kocaefe's gas model was used. The calculated heat fluxes at the wall have been compared with experimental measurements taken on the boiler for three sets of operating conditions, and they indicated that confidence can be placed in the results.

The comparisons and evaluations of the predictions obtained by those concepts [27,28] with the results of other gas radiative properties models are difficult because the codes [27,28] did not deal with radiation only. Those 3-D codes link fluid flow, turbulence model, combustion pattern, heat transfer by convection, conduction and radiation, anisotropic particles scattering and gas radiative properties models. Thus it was very difficult here to carry out the analysis of the role played only by the gas radiative properties models.

Coelho [29] has carried out 3-D numerical simulations of radiative heat transfer from non-gray gases by the DOM and DTM. He has used several gas radiative properties models as CK, SLW and WSGG models. The predictions were compared against the ray tracing SNB results [30] that were used as benchmark data. Coelho has concluded, inter alia, the following: (1) The WSGGM is computationally economical and has moderate accuracy. (2) The SLW model is a compromise between accuracy and numerical requirements but it needs additional work for an optimization of the coefficients. (3) The CK model is the most accurate but too time consuming for engineering applications. The study of 3-D non-gray radiation was performed using the SNB model [30]. The updated band parameters were used [31]. The exact narrow-band averaged RTE was solved by a ray-tracing method. The results were presented for non-gray gas radiation in a 3-D rectangular geometry for three different gas mixtures. One of the conclusions was that the method is very time-consuming and not recommended for other applications. It was developed only for the purpose of obtaining accurate results by the solution of the narrow-band averaged RTE in 3-D geometries. The results are precious and will be used as benchmark for future evaluations of other 3-D non-gray gas radiation models.

The comparison of the predictions calculated by nine total emissivity models against the calculations done by exponential wide band model (EWBM) was carried out [3]. One of the main conclusions was that Smith et al. weighted sum of gray gases model [19] indicates the advantage.

The aims of this study were to develop a new 3-D non-gray gas mathematical model and computer code for radiation, based on the coupling of FVM and weighted sum of gray gases model (WSGGM) convenient for incorporation within CFD codes. The FVM and WSGGM have not been previously combined to the author's best knowledge. Smith et al.'s WSGGM, showing the advantage compared with others, was incorporated in this model. One of the goals of this work was to obtain the model that will avoid the drawbacks of spectral line and bands gas models. It was believed that the model developed here will be reasonable accurate, convenient for wide engineering applications and suitable for incorporation and work within CFD codes.

2. Mathematical formulations

2.1. Radiative transfer equation for a gray gas

The equation for radiative heat transfer for a gray medium has been presented in many sources, Ozisik [4], Siegel and Howell [32] and Modest [38], as

$$\frac{\mathrm{d}I(\vec{r},\hat{s})}{\mathrm{d}s} = -\beta(\vec{r})I(\vec{r},\hat{s}) + S(\vec{r},\hat{s}). \tag{1}$$

This equation indicates that the change of radiant intensity I takes place along a length ds. The equation simply states that the change of intensity along a path, or the energy accumulation, is equal to the difference between the energy gained and energy lost. Here the term $-\beta(\vec{r})I(\vec{r},\hat{s})$ accounts for attenuation and $S(\vec{r},\hat{s})$ for augmentation.

The extinction coefficient β, is written as

$$\beta(\vec{r}) = \kappa(\vec{r}) + \sigma(\vec{r}), \tag{2}$$

where $\kappa(\vec{r})$ represents the absorption of radiant energy and $\sigma(\vec{r})$ accounts for the out-scattering of radiant energy.

The energy source function, $S(\vec{r},\hat{s})$, is given as

$$S(\vec{r},\hat{s}) = \kappa(\vec{r})I_{\mathrm{b}}(\vec{r}) + \frac{\sigma(\vec{r})}{4\pi}\int_{4\pi} I(\vec{r},\hat{s})\Phi(\hat{s}',\hat{s})\,\mathrm{d}\Omega'. \tag{3}$$

The first term in this expression, $\kappa(\vec{r})I_{\mathrm{b}}(\vec{r})$, represents gas emission while the second term accounts for the accumulation of radiant energy due to in-scattering from all other directions in the domain.

Radiant intensity I depends on spatial position $\vec{r}$ and angular direction $\hat{s}$. For 2-D rectangular enclosure, I depends on four spatial variables, $I(x,y,\theta,\phi)$ and for a 3-D enclosure, on five spatial variables, $I(x,y,z,\theta,\phi)$. Here x, y, z are the Cartesian coordinates of the position vector, $\vec{r}$, and θ, ϕ are the polar and planar angles, respectively, that define the intensity direction $\hat{s}(\theta,\phi)$.

2.2. Boundary condition for an opaque diffuse surface expressed as the boundary intensity defined for a gray gas

The boundary condition for an opaque diffuse surface, given in the form of the boundary intensity, is

$$I(\vec{r},\hat{s}) = \varepsilon(\vec{r})I_{\mathrm{b}}(\vec{r}) + \frac{\rho(\vec{r})}{\pi}\int_{\hat{s}'\cdot\hat{n}<0} I(\vec{r},\hat{s}')|\hat{s}'\cdot\vec{n}|\,\mathrm{d}\Omega'. \tag{4}$$

The first term on the right hand side of this equation is the emission due the surface temperature, the so-called black-body radiation. The second term represents the reflection of the incoming intensity. The radiant energy leaving an opaque diffuse surface is just the sum of these two effects.

2.3. Radiative heat transfer relations for a gray gas

Besides the radiant intensities and the above written equations, additional quantities and expressions should be defined. The incident radiation coming from all directions (i.e., integrated over 4π radians) is

$$G(\vec{r}) = \int_{4\pi} I(\vec{r},\hat{s})\,\mathrm{d}\Omega. \tag{5}$$

The radiative heat flux in the direction of the unit vector $\hat{i}$ is expressed as

$$q_i(\vec{r}) = \int_{4\pi} I(\vec{r},\hat{s})(\hat{s}\cdot\hat{i})\,\mathrm{d}\Omega. \tag{6}$$

Using this, the radiative heat fluxes in x, y and z directions are

$$q_x(\vec{r}) = \int_{4\pi} I(\vec{r},\hat{s})(\hat{s}\cdot\hat{e}_x)\,\mathrm{d}\Omega, \tag{7}$$

$$q_y(\vec{r}) = \int_{4\pi} I(\vec{r},\hat{s})(\hat{s}\cdot\hat{e}_y)\,\mathrm{d}\Omega, \tag{8}$$

$$q_z(\vec{r}) = \int_{4\pi} I(\vec{r},\hat{s})(\hat{s}\cdot\hat{e}_z)\,\mathrm{d}\Omega. \tag{9}$$

The angular direction is defined by the unit vector

$$\hat{s} = (\sin\theta\cos\phi)\hat{e}_x + (\sin\theta\sin\phi)\hat{e}_y + (\cos\theta)\hat{e}_z. \tag{10}$$

The radiation source-sink term for a gray absorbing, emitting and scattering medium is given as

$$\kappa(\vec{r})\int_{4\pi}[I(\vec{r},\hat{s}) - I_{\mathrm{b}}(\vec{r})]\,\mathrm{d}\Omega. \tag{11}$$

The first term under the integral is the incident radiation and the second term is the emission due to the gas temperature, or black-body radiation.

If the absorption coefficient $\kappa(\vec{r})$ does not depend on position $\vec{r}$, then

$$\kappa(\vec{r}) = \kappa. \tag{12}$$

Eq. (11) can be written as

$$\kappa\left[\int_{4\pi} I(\vec{r},\hat{s})\,\mathrm{d}\Omega - \int_{4\pi} I_{\mathrm{b}}(\vec{r})\,\mathrm{d}\Omega\right]. \tag{13}$$

The first integral in the brackets of Eq. (13) is the incident radiation given by Eq. (5) as $G(\vec{r})$. In the second integral, since the term $I_{\mathrm{b}}(\vec{r})$ (representing black-body radiation which can be expressed as σT^4) does not depend on the directions Ω, this integral after integration can be written as

$$\int_{4\pi} I_{\mathrm{b}}(\vec{r})\,\mathrm{d}\Omega = I_{\mathrm{b}}(\vec{r})\int_{4\pi}\mathrm{d}\Omega = 4\pi I_{\mathrm{b}}(\vec{r}). \tag{14}$$

After these transformations the source-sink term, Eq. (11), can be expressed as

$$\kappa[G(\vec{r}) - 4\pi I_b(\vec{r})]. \quad (15)$$

Eq. (15), conventionally taken with a negative sign in the literature [38], is the divergence of the radiative heat flux, designated by $\nabla \cdot q$:

$$\nabla \cdot q = \kappa[4\pi I_b(\vec{r}) - G(\vec{r})]. \quad (16)$$

2.4. Total gas emissivity and absorptivity

The word "total" is used here to stress that the gas emissivity and absorptivity are defined for the whole region of wavelengths rather than for a particular value of wavelength. The variables defined for a specific value of wavelength are called monochromatic or spectral variables.

The variables required to define total gas emissivity and absorptivity are as follows respectively:

$$\varepsilon_g = f_1(L, p, P, C, T_g), \quad (17)$$

$$\alpha_{gs} = f_2(L, p, P, C, T_g, T_s). \quad (18)$$

The dependencies of the total gas emissivity and absorptivity on all these variables are very complex and they have not been expressed by explicit and convenient mathematical expressions so far.

Here C is the composition of the gas. It is included to show the effect of colliding molecules for different species. It should be mentioned that the total absorptivity depends on the same variables as the total emissivity plus the irradiation temperature of surfaces surrounding the gas is also introduced.

2.5. Weighted sum of gray gases model (WSGGM)

There are several gas radiative properties models, called global models, that development were based on the concept of weighted sum of gray gases. They are Hottel and Sarofim's gas radiative properties model [2], Steward and Kocaefe's model [17,18], Smith et al.'s WSGG model [19] etc. Within the model and computer codes developed here, the Smith et al.'s WSGG model [19] was incorporated.

The following equation is used for the evaluation of total emissivity for the WSGGM:

$$\varepsilon = \sum_{i=0}^{I} a_{\varepsilon,i}(T)[1 - e^{-\kappa_i PS}], \quad (19)$$

where $a_{\varepsilon,i}$ is the emissivity weighting factors for the gray gas i. The weighting factors are dependent on gas temperature T. The expression in the brackets in Eq. (19) is the ith gray gas emissivity, having absorption coefficient κ_i, partial pressure P and the thickness of gas layer, or path length S. For a gas mixture P is the sum of partial pressures of absorbing gases. The physical interpretation of the weighting factor $a_{\varepsilon,i}$ is the fractional amount of black-body energy in the regions of spectrum where gray gas having absorption coefficient κ_i exists. A value of zero is assigned to absorption coefficient for $i = 0$. This gas is called "clear gas". It accounts for windows in the spectrum between the spectral regions that have absorption. The total emissivity is an increasing function of partial pressure–path length product approaching unity in the limit. Therefore the weighting factors must sum to unity and also must have positive values. The weighting factor for clear gas, i.e. for $i = 0$, is defined as

$$a_{\varepsilon,0}(T) = 1 - \sum_{i=1}^{I} a_{\varepsilon,i}. \quad (20)$$

So, I values of the weighting factors should be evaluated. A very common and convenient representation of the temperature dependency of the weighting factors is a polynomial of order $J - 1$ given as

$$a_{\varepsilon,i}(T) = \sum_{j=1}^{J} b_{\varepsilon,i,j} T^{j-1}. \quad (21)$$

Here $b_{\varepsilon,i,j}$ are referred to as the emissivity gas temperature polynomial coefficients. The absorption coefficients κ_i and the polynomial coefficients $b_{\varepsilon,i,j}$ are obtained by fitting Eq. (19) to a table of total emissivities previously calculated from the EWBM. (The total emissivities for various gas mixtures can be obtained by different means: by experimental measurements, by calculation based on spectral lines or bands based on Hottel's charts [2] etc.) Having I gray gases and $J - 1$ polynomial order, $I(J - 1)$ coefficients should be evaluated. For total absorptivity, the irradiation temperature of surfaces surrounding the gas, T_s, must be also taken into account. So the expression for total absorptivity is

$$\alpha = \sum_{i=0}^{I} a_{\alpha,i}(T, T_s)[1 - e^{-\kappa_i PS}]. \quad (22)$$

Here the absorptivity weighting factors,$a_{\alpha,i}$, are the functions of gas temperature, T, and of surface irradiation temperature, T_s, as well. The weighting factors must be positive and the sum of all weighting factors must be equal to unity. The value of weighting factor for $i = 0$ is evaluated as

$$a_{\alpha,0} = 1 - \sum_{i=1}^{I} a_{\alpha,i}. \quad (23)$$

The dependency of the weighting factors on gas and irradiation temperatures is expressed by polynomials of orders $J - 1$ and $K - 1$, respectively as

$$a_{\alpha,i} = \sum_{j=1}^{J} \left[\sum_{k=1}^{K} c_{\alpha,i,j,k} T_s^{k-1} \right] T^{j-1}, \quad (24)$$

where $c_{\alpha,i,j,k}$ are the absorptivity polynomial coefficients. The absorption coefficients, κ_i, for total emissivity and

absorptivity are taken to be identical in order to reduce the computational efforts. But the orders of polynomials for emissivity and absorptivity may differ. The number of coefficients needed for total absorptivity is equal to $I * J * K$.

One issue should be stressed here. Irradiation temperature T_s plays important role for the evaluation of total gas absorptivity, or in this model for the evaluation of absorptivity weighting factors. The significance of irradiation temperature is emphasized by Smith et al. [19]. Hottel and Sarofim [37] discarded the gas temperature polynomial and selected a mean gas temperature for calculation of gas absorptivity. In their model, they reported only polynomial coefficients to take into account the effect of the irradiation temperature.

2.6. Modification of general RTE in order to be used coupled with WSGGM

The general integral–differential RTE, valid when radiation is modeled only with one gray gas, is modified in order to be linked with WSGGM. A new set of RTE-s is derived. The weighting factors for gas emissivities and gas absorptivities, defined by WSGGM are introduced in these equations. Each of the gray gases is represented with a separate RTE.

Substituting Eq. (3) into Eq. (1), the RTE when the radiant energy is transferred within only that one gray gas is expressed as follows:

$$\frac{\mathrm{d}I(\vec{r},\hat{s})}{\mathrm{d}s} = -\beta(\vec{r})I(\vec{r},\hat{s}) + \kappa(\vec{r})I_\mathrm{b}(\vec{r}) + \frac{\sigma(\vec{r})}{4\pi}\int_{4\pi} I(\vec{r},\hat{s})\Phi(\hat{s}',\hat{s})\,\mathrm{d}\Omega'. \tag{25}$$

The link between RTE for only one gray gas with WSGGM is based on the concept that for each gray gas is used one RTE. Instead of using only one gray gas and only one RTE for the transfer of radiant energy, the radiant energy will be transferred now via, or through 'I' gray gases. They are known and called as $I-1$ gray gases plus one clear gas used for the windows in spectrum. So I different "channels", regions or domains of wavelengths, will be used for the exchange of radiative energy, and they will not interfere between themselves.

Thus, RTE for one gray gas, when the radiant energy is modeled by the means of more gray gases or by WSGGM, is expressed as follows:

$$\frac{\mathrm{d}I_{\mathrm{g},i}(\vec{r},\hat{s})}{\mathrm{d}s} = -\beta_{\mathrm{g},i}(\vec{r})I_{\mathrm{g},i}(\vec{r},\hat{s}) + \kappa_{\mathrm{g},i}(\vec{r})I_\mathrm{b}(\vec{r})a_{\varepsilon,i}(T) + \frac{\sigma(\vec{r})}{4\pi}\int_{4\pi} I_{\mathrm{g},i}(\vec{r},\hat{s}')\Phi(\hat{s}',\hat{s})\,\mathrm{d}\Omega'. \tag{26}$$

Here the extinction coefficient is given as

$$\beta_{\mathrm{g},i}(\vec{r}) = \kappa_{\mathrm{g},i}(\vec{r}) + \sigma(\vec{r}). \tag{27}$$

The expression $a_{\varepsilon,i}(T)$ is the emissivity weighting factor discussed previously in Section 2.5. The physical interpretation of the weighting factor $a_{\varepsilon,i}$ is the fractional amount of black-body energy in the regions of spectrum where gray gas having absorption coefficient κ_i exists. So wherever the black-body radiation was in RTE used for modeling by only one gray gas, in this concept must be weighted by weighting factors.

Thus, in this concept, instead of solving one RTE, the I RTE-s will be solved, one for each gray gases. So I different intensities, $I_{\mathrm{g},i}(\vec{r},\hat{s})$, will be calculated.

It should be kept in mind that letter I here is used as the total number of gray gases and as the designation for radiation intensity, but they have nothing in common.

Instead of boundary condition given by Eq. (4), when the radiant energy is considered by only one gray gas, the boundary condition in this case, when the radiant energy is modeled by the means of more gray gases, i.e. by WSGGM, for a gray gas, for an opaque diffuse surface and if BC is given as the boundary intensity, is expressed as follows:

$$I_{\mathrm{g},i}(\vec{r},\hat{s}) = \varepsilon(\vec{r})I_\mathrm{b}(\vec{r})a_{\alpha,i}(T,T_\mathrm{s}) + \frac{\rho(\vec{r})}{\pi} \times \int_{\hat{s}'\cdot\hat{n}<0} I_{\mathrm{g},i}(\vec{r},\hat{s}')|\hat{s}'\cdot\vec{n}|\mathrm{d}\Omega'. \tag{28}$$

Instead of radiative source-sink term given by Eq. (11), when the radiant energy is transferred via only one gray gas, the source-sink term for a gray absorbing, emitting and scattering medium in this case, when the radiant energy is modeled by the means of more gray gases, i.e. by WSGGM, is expressed as follows:

$$\kappa_{\mathrm{g},i}(\vec{r})\int_{4\pi}[I_{\mathrm{g},i}(\vec{r},\hat{s}) - a_{\varepsilon,i}(T)I_\mathrm{b}(\vec{r})]\,\mathrm{d}\Omega. \tag{29}$$

The total source-sink term, when WSGGM with I gray gases is applied, is equal to the sum of source-sink terms given by Eq. (29), i.e. evaluated for each of the gray gases, and is expressed as follows:

$$\sum_{i=1}^{I}\kappa_{\mathrm{g},i}(\vec{r})\int_{4\pi}[I_{\mathrm{g},i}(\vec{r},\hat{s}) - a_{\varepsilon,i}(T)I_\mathrm{b}(\vec{r})]\,\mathrm{d}\Omega. \tag{30}$$

Using the basic concept of WSGG where the total radiative energy is transferred via I different regions of wavelength, here I is the total number of gray gases, and summing Eq. (26) over i, i.e. summing both, left and right hand sides of that equation over i, gives the following expression:

$$\sum_{i=1}^{I}\frac{\mathrm{d}I_{\mathrm{g},i}(\vec{r},\hat{s})}{\mathrm{d}s} = -\sum_{i=1}^{I}\beta_{\mathrm{g},i}(\vec{r})I_{\mathrm{g},i}(\vec{r},\hat{s}) + \sum_{i=1}^{I}\kappa_{\mathrm{g},i}(\vec{r})I_\mathrm{b}(\vec{r})a_{\varepsilon,i}(T) + \sum_{i=1}^{I}\frac{\sigma(\vec{r})}{4\pi}\int_{4\pi} I_{\mathrm{g},i}(\vec{r},\hat{s})\Phi(\hat{s}',\hat{s})\,\mathrm{d}\Omega'. \tag{31}$$

For only one gray gas ($I = 1$) Eq. (31) becomes Eq. (25). The comparison of Eq. (31) derived for gas radiative properties models based on WSGG, or for so-called global models, against Eq. (25) that is general RTE, valid for monochromatic and only for one gray gas cases, shows that Eq. (31) satisfies Eq. (25) because the basic physical concepts of WSGG are satisfied. They are as follows:

1. Left hand side of Eq. (31),

$$\sum_{i=1}^{I} \frac{\mathrm{d}I_{\mathrm{g},i}(\vec{r},\hat{s})}{\mathrm{d}s}, \tag{32}$$

means that the total change of intensity or the total accumulation of radiant energy along the path length ds for I gray gases is equal to the sum of intensity changes for each of the gray gases.

2. First member of right hand side of Eq. (31),

$$-\sum_{i=1}^{I} \beta_{\mathrm{g},i}(\vec{r}) I_{\mathrm{g},i}(\vec{r},\hat{s}) \tag{33}$$

shows that total attenuation, or the total radiative energy absorbed and out-scattered for I gray gases is equal to the sum of attenuations for each of the gray gases.

3. Second member of right hand side of Eq. (31),

$$\sum_{i=1}^{I} \kappa_{\mathrm{g},i}(\vec{r}) I_{\mathrm{b}}(\vec{r}) a_{\varepsilon,i}(T), \tag{34}$$

means that the total black-body radiation or the total gas emission for I gray gases is equal to the sum of gas emissions for each of the gray gases.

4. Third or last member of right hand side of Eq. (31),

$$\sum_{i=1}^{I} \frac{\sigma(\vec{r})}{4\pi} \int_{4\pi} I_{\mathrm{g},i}(\vec{r},\hat{s}) \Phi(\hat{s}',\hat{s})\, \mathrm{d}\Omega', \tag{35}$$

indicates that total in-scattering, or the total in-scattered energy for I gray gases is equal to the sum of in-scatterings for each of the gray gases.

The following should be mentioned here. The concept where the total radiative energy, "total" here means within the whole relevant region of spectrum, was transferred by WSGG has been applied in a similar way previously [27,28]. In that case the Hottel and Cohen zone method and Monte Carlo method, that is a kind of solution of RTE, was coupled with two different WSGG models, i.e. coupled with (1) Hottel and Sarofim's [2] and (2) Steward and Kocaefe's gas radiative properties models [17,18]. The basic approach that the total transferred radiative energy within the relevant spectrum is equal to the sum of radiative energies transferred by each spectral region of gray gases is the same in both cases, i.e. in studies [27,28] and in this work. But the solution method of RTE and the WSGG model are different in this work. Here the solution of RTE is by FVM and is coupled with Smith et al.'s WSGG model [19]. To the author's best knowledge it is a novel concept not published previously.

2.7. Modified radiative heat transfer relations to be used for WSGG

The total incident radiation coming from all directions (i.e., integrated over 4π radians) for all, i.e. I, gray gases, is equal to the sum of incident radiations for each of the gray gases or

$$G_{\mathrm{tot}}(\vec{r}) = \sum_{i=1}^{I} G_{\mathrm{g},i}(\vec{r}) = \sum_{i=1}^{I} \int_{4\pi} I_{\mathrm{g},i}(\vec{r},\hat{s})\, \mathrm{d}\Omega. \tag{36}$$

The total radiative heat flux, i.e. for all gray gases, in the direction of the unit vector $\hat{i}$ is expressed as the sum of heat fluxes for each of the gray gases in the direction of the unit vector $\hat{i}$ or as

$$q_{\hat{i},\mathrm{tot}}(\vec{r}) = \sum_{i=1}^{I} q_{\hat{i},\mathrm{g},i}(\vec{r}) = \sum_{i=1}^{I} \int_{4\pi} I_{\mathrm{g},i}(\vec{r},\hat{s})(\hat{s}\cdot\hat{i})\, \mathrm{d}\Omega. \tag{37}$$

Here unit vector $\hat{i}$ taken for $\hat{i}$ direction should be distinguished from index i that is used for the designation of ith gray gas.

Using, Eq. (37) radiative heat fluxes in x, y and z directions are respectively

$$q_{x,\mathrm{tot}}(\vec{r}) = \sum_{i=1}^{I} q_{x,\mathrm{g},i}(\vec{r}) = \sum_{i=1}^{I} \int_{4\pi} I_{\mathrm{g},i}(\vec{r},\hat{s})(\hat{s}\cdot\hat{e}_x)\, \mathrm{d}\Omega, \tag{38}$$

$$q_{y,\mathrm{tot}}(\vec{r}) = \sum_{i=1}^{I} q_{y,\mathrm{g},i}(\vec{r}) = \sum_{i=1}^{I} \int_{4\pi} I_{\mathrm{g},i}(\vec{r},\hat{s})(\hat{s}\cdot\hat{e}_y)\, \mathrm{d}\Omega, \tag{39}$$

$$q_{z,\mathrm{tot}}(\vec{r}) = \sum_{i=1}^{I} q_{z,\mathrm{g},i}(\vec{r}) = \sum_{i=1}^{I} \int_{4\pi} I_{\mathrm{g},i}(\vec{r},\hat{s})(\hat{s}\cdot\hat{e}_z)\, \mathrm{d}\Omega. \tag{40}$$

After integration of Eq. (30) the total source-sink term is

$$\sum_{i-1}^{I} \kappa_{\mathrm{g},i}[G_{\mathrm{g},i}(\vec{r}) - 4\pi a_{\varepsilon,i}(T) I_{\mathrm{b}}(\vec{r})]. \tag{41}$$

The total divergence of the radiative heat flux is equal to the sum of the divergences for each of the gray gases:

$$\begin{aligned} \nabla\cdot q_{\mathrm{tot}} &= \sum_{i=1}^{I} \nabla\cdot q_{\mathrm{g},i} \\ &= \sum_{i=1}^{I} \kappa_{\mathrm{g},i}[4\pi a_{\varepsilon,i}(T) I_{\mathrm{b}}(\vec{r}) - G_{\mathrm{g},i}(\vec{r})]. \end{aligned} \tag{42}$$

3. Numerical features

The new original computer codes that solve RTE in 2-D and 3-D Cartesian coordinates based on FVM are developed. Detailed and thorough discussion of FVM and of discretization procedure used in this study is given in literature [33–35] and it will not be discussed again.

Before the work was continued towards non-gray-gas mathematical modeling, it was necessary to test firstly developed one gray gas codes. For the sake of testing previously developed 2-D and 3-D codes for one gray gas, the predictions of those codes were compared against the results of Chai [33], Chai et al. [34] and Raithby and Chui [36] and the agreements between them are excellent. The predictions are almost identical with those results.

The spatial differencing scheme used in this work to relate the boundary intensities to nodal intensities is step scheme. This scheme sets the downstream boundary intensities equal to the upstream nodal intensities.

The process of intensity calculation is repeated for all specified intensity directions and a solution is considered converged when it satisfies the following criterion:

$$|I_P^l - I_P^{l0}|/I_P^l \leqslant 10^{-6}. \tag{43}$$

Here I_P^l is the latest and I_P^{l0} the previous iteration.

The scheme appeared to be very efficient. The guess of initial intensity field is set to zero. The solution converges very fast. For the particular cases of 2-D geometry and for one gray gas, the incident heat flux to the accuracy of six decimal points is achieved only within a single iteration. But it should be mentioned that, for 2-D geometry, within an iteration, the code has four sweeps, each of which in one of four "quadrant directions". For the test cases performed here, which are 3-D and for non-gray gases, the accuracy of six decimal points is achieved within two iterations. Here, for 3-D geometry, within an iteration the code has eight sweeps, each of which in one of eight "vertex directions".

For non-gray gas intensity calculations, the convergence is deemed finished when the criterion given by Eq. (43) is satisfied for each of the gray gases.

4. Description of test problems

Detailed description of test problems is given in Liu's paper [30]. Those results, obtained by SNB model, are considered as the most accurate and used here as the benchmark. There are three test cases. To test the mathematical model and computer code developed here, the comparisons were performed against two test cases, case 1 and case 3. The further predictions by this model are continued for a new case, not previously published, and designated here as the test case 4. The geometry considered for all test cases, for old cases 1 and 3 and for new case 4, consists of a 3-D rectangular enclosure having the dimensions 2 m×2 m×4 m. All the surrounding walls are black and cold, i.e. at 300 K. The enclosure contains the gas mixture at atmospheric pressure, i.e. at 1 atm.

In the test case 1 the gas mixture composition is uniform and consists of pure water vapor. The temperature field of the gas is kept uniform at 1000 K.

In the test case 3 the medium composition is a uniform gas mixture of 10% CO_2, 20% H_2O and 70% N_2 on a molar basis. The temperature field of the gas is non-uniform and symmetrical about the centerline of the enclosure. These temperatures are expressed by the expression $T = (T_c - T_e)f(r/R) + T_e$. Here T_c is the gas temperature along the centerline of the enclosure and T_e is the exit temperature at $z = 4$ m. The centerline temperature T_c is taken to increase linearly from 400 K at the inlet ($z = 0$) to maximal value of 1800 K at $z = 0.375$ m and then decreases linearly to 800 K at the exit ($z = 4$ m). Inside the enclosure a circular region or a cylinder around the centerline can be imagined, where $R = 1$ m is the radius of cylinder. The variation of gas temperature inside the circular region of the cross section enclosure is given by equation $f(r/R) = 1 - 3(r/R)^2 + 2(r/R)^3$ where r is the distance from the centerline of the enclosure. The gas temperatures outside the circular region, i.e. between the cylinder with radius $R = 1$ m and the walls of rectangular enclosure were defined as uniform and equal to the value of exit temperature $T_e = 800$ K.

In new calculation case, designated as case 4, all the conditions and input parameters are the same as for test case 3, except the gas mixture that is now 10% CO_2, 10% H_2O and 80% N_2 on a molar basis. Here the ratio of partial pressures of water vapor and carbon dioxide is equal to unity ($p_w/p_c = 1$). The Smith et al.'s WSGG model with "4 gray gases + one clear gas" is applied.

Here should be emphasized that, strictly speaking, the selected test cases 1 and 3 [30] are not the best or adequate to be used as the benchmark for the comparisons against the predictions obtained by this particular WSGG model. This is because the calculations in benchmark [30] are performed for wall temperature set at $T_s = 300$ K, while the WSGG model [19] used here is developed for the region of irradiation temperatures $600 < T_s < 2400$ K. This benchmark was only available. Author, same as others [30], did not find in literature any other values of non-gray gas radiation in 3-D geometry within the irradiation region of $600 < T_s < 2400$ K that could be used for comparison.

In addition the irradiation temperature $T_s = 300$ K used in all these test cases is artificial and does not coincide with engineering problems. The irradiation temperatures of 600 K and higher are common and very realistic surface temperatures for the majority of

industrial combustion chambers and furnaces. Therefore in future calculation cases, to be used for comparisons by others, the surface or wall temperature should be set at $T_s = 600$ K.

5. Results and discussion

The model and code developed here were applied to test cases 1 and 3 previously simulated by others [30] and [29], as well as to a new case designated as test case 4. Also two various spatial grid sizes and three angular discretizations in polar and azimuthal directions were used to analyze their effects on the predictions accuracy.

For test case 1 the predictions performed by WSGG model with "3 gray gases + 1 clear gas" are shown in Fig. 1(a)–(d). The rectangular grid for these predictions is $25 \times 25 \times 25$. The angular discretization is 4×20, i.e. it consists of 4 increments in polar and 20 increments in azimuthal directions.

In Fig. 1(a) the radiative heat source along centerline (1 m, 1 m, z) for test case 1, predicted by new model i.e. by FVM with WSGGM, as well as the results calculated by (i) ray tracing with SNB [30] and (ii) DOM with WSGG [29] are presented. In Fig. 1(b) the incident heat flux along (2 m, 1 m, z) for test case 1, predicted by new model and the results calculated by (i) ray tracing with SNB [30] and (ii) DOM with WSGG [29] are presented. In Fig. 1(c) the radiative heat source along (x, 1 m, 0.375 m) for test case 1, predicted by the new model as well as the results calculated by (i) ray tracing with SNB [30] and (ii) DOM with WSGG [29] are presented. In Fig. 1(d) the incident heat flux along (x, 1 m, 4 m) for test case 1, predicted by the new model and the results cal-

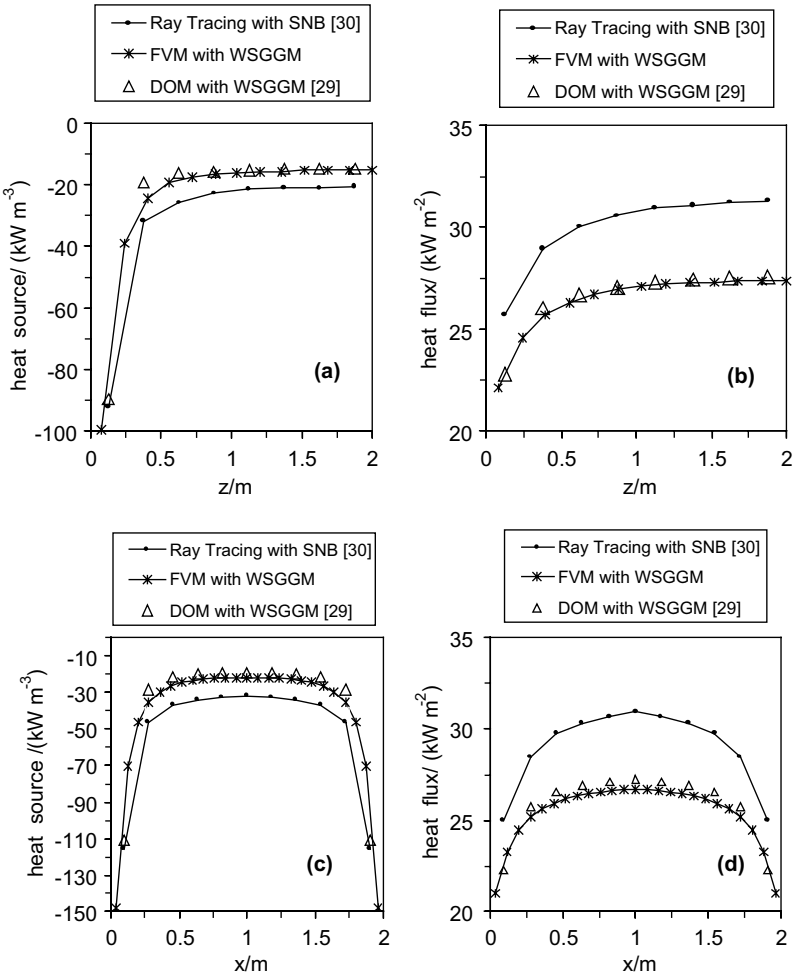

Fig. 1. Predictions of radiative heat source and incident heat flux and their comparisons against (i) ray tracing with SNB [30] and (ii) DOM with WSGG [29] for test case 1: (a) radiative heat source along the centerline (1 m, 1 m, z); (b) incident heat flux along (2 m, 1 m, z); (c) radiative heat source along (x, 1 m, 0.375 m); (d) incident heat flux along (x, 1 m, 4 m).

culated by (i) ray tracing with SNB [30] and (ii) DOM with WSGG [29] are presented. The rectangular grid used for new predictions differs from grids in papers [30] and [29].

It can be seen in Fig. 1(a) and (c) that the new model predictions of radiative heat source are very close to, or almost identical with, the values calculated by Coelho [29] by DOM with WSGG. Compared against benchmark [30], both of them, the new results and Coelho's values [29] are under-predicted by absolute values (because the predictions were taken with negative i.e. minus sign) approximately to the same extent. Fig. 1(b) and (d) shows that the new model predictions of incident heat flux are again very close to, or almost the same as, the values calculated by Coelho [29] by DOM with WSGG. Compared against benchmark [30], both of them, the new results and Coelho's values are underestimated.

For test case 3 the predictions are shown in Fig. 2(a) and (b). The spatial rectangular grid for these predictions is $41\times41\times80$. The angular discretization consists of 4 increments in polar and 20 increments in azimuthal directions.

In Fig. 2(a) the radiative heat source along centerline (1 m, 1 m, z) for test case 3, predicted by the new model with "3 gray gases + 1 clear gas" (4gg) and with "4 gray gases + 1 clear gas" (5gg) as well as the results calculated by (i) ray tracing with SNB [30] and (ii) DOM with WSGG [29] are presented. In Fig. 2(b) the incident heat flux along (2 m, 1 m, z) for test case 3, predicted by the new model with 4gg and with 5gg as well as the results calculated by (i) ray tracing with SNB [30] and (ii) DOM with WSGG [29] are presented.

Fig. 2(a) shows that the predictions of radiative heat source obtained by 5gg, plotted by square symbols, are the closest to the benchmark, i.e. they are the most accurate. They are significantly more accurate than the predictions calculated by 4gg, plotted by dash line. The 4gg predictions of heat source, plotted by dash line, are very close or almost identical with results obtained by DOM with WSGGM [29] that are plotted by triangle symbols. It could be expected because the DOM and the FVM are very similar methods and in [29] also 4gg WSGG model was used.

Fig. 2(b) shows that the predictions of incident heat flux calculated by 4gg, plotted by dash line, and calculated by 5gg, plotted by square symbols, little differ. The predictions of heat flux calculated by FVM with WSGGM and by DOM with WSGGM [29] are close to each other. Only in the narrow region of highest value of incident heat flux, the heat flux calculated by DOM with WSGGM [29] are closer to ray tracing with SNB [30] results than the predictions calculated by FVM with WSGGM. The explanation for this depends on the knowledge whether and how the authors in [29] and [30] did apply irradiation temperature $T_s = 300$ K for gas absorptivity evaluation.

In Fig. 3(a) the effect of spatial grid on the accuracy of the radiative source term along centerline (1 m, 1 m, z) for test case 3 were analyzed. The predictions were carried out for two rectangular uniform grids $25\times25\times25$ and $41\times41\times80$ and for WSGGM with 4 and with 5 gray gases. It appears that the predictions are not sensitive on these grid sizes. The only differences were caused due to the numbers of gray gasses.

The same grid sizes $25\times25\times25$ and $41\times41\times80$ with 4 and 5 gray gases models were used for the predictions of incident heat flux along (2 m, 1 m, z) for test case 3. These results are given in Fig. 3(b). Comparing the

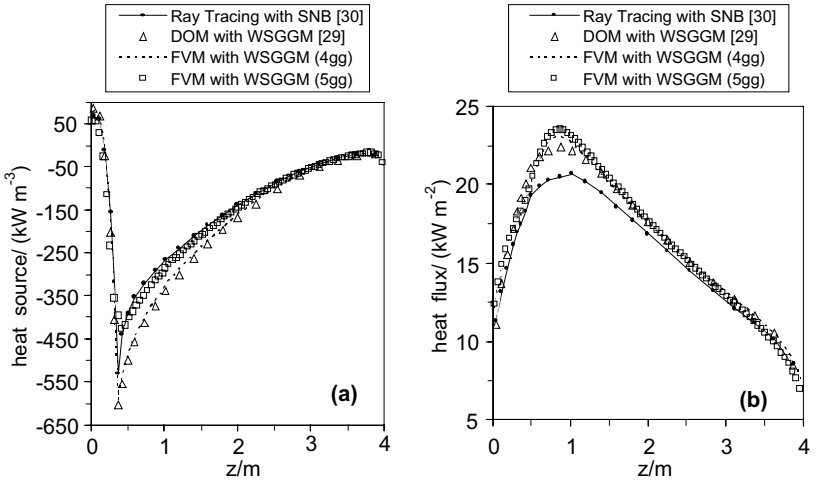

Fig. 2. Predictions of radiative heat source and incident heat flux and their comparisons against (i) ray tracing with SNB [30] and (ii) DOM with WSGG [29] for test case 3: (a) radiative heat source along the centerline (1 m, 1 m, z); (b) incident heat flux along (2 m, 1 m, z).

predictions of heat flux for 4gg model, calculated by grid $25\times25\times25$, plotted by square symbols, and heat flux calculated by grid $41\times41\times80$, plotted by full line, it can be seen that minor differences occur. By comparison the heat flux results for 5 gray gases model with grid $25\times25\times25$, plotted by "+" (plus) symbols, against heat flux calculated by grid $41\times41\times80$, plotted by dash line, the differences are even smaller and more insignificant than for 4 gray gases. Those predictions can be considered as grid independent as the comparisons in Fig. 3(a) and (b) show that. For that case the uniform grid $25\times25\times25$ is satisfactory. Even a coarse grid as $11\times11\times16$ that is used in [30] and [29] gave almost the same predictions as a finer grid with increments $17\times17\times32$.

Fig. 3(c) and (d) shows the effect of angular discretization on the radiative heat source along centerline (1 m, 1 m, z) and on the incident heat flux along (2 m, 1 m, z) respectively for test case 3. The uniform rectangular grid $25\times25\times25$ was used. The four gray gases (4gg) model was applied. Three various angular discretizations having the number of increments in polar and azimuthal directions 4×20, 8×40 and 16×80, respectively were used. It can be seen in Fig. 3(c) and (d) that, both, radiative heat source and incident heat flux respectively show so small sensitivity to the angular discretization, that it practically can be neglected. Thus all the predictions presented in Figs. 1(a)–(d) and 2(a) and (b) were carried out with polar and azimuthal discretization 4×20, respectively.

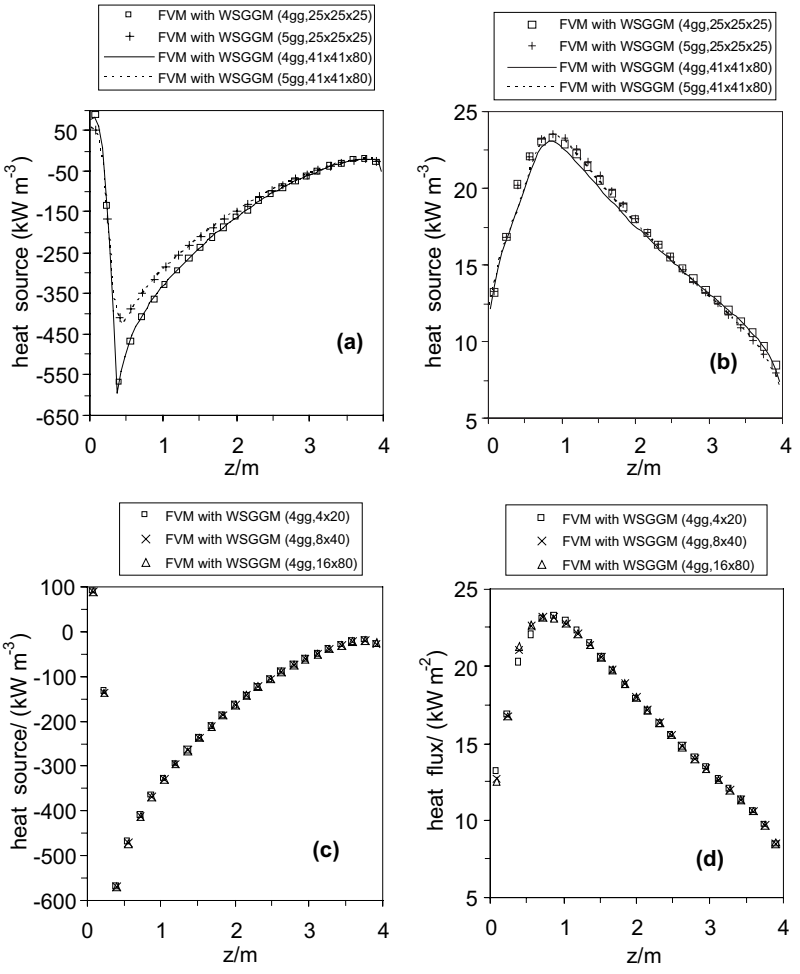

Fig. 3. Influence of spatial grid size and angular discretization on radiative heat source and on incident heat flux for test case 3: (a) comparison of radiative heat sources for two different grid sizes and for the models with 4 and 5 gray gases; (b) comparison of incident heat fluxes for two different grid sizes and for the models with 4 and 5 gray gases; (c) comparison of radiative heat sources for three different angular discretizations; (d) comparison of incident heat fluxes for three different angular discretizations.

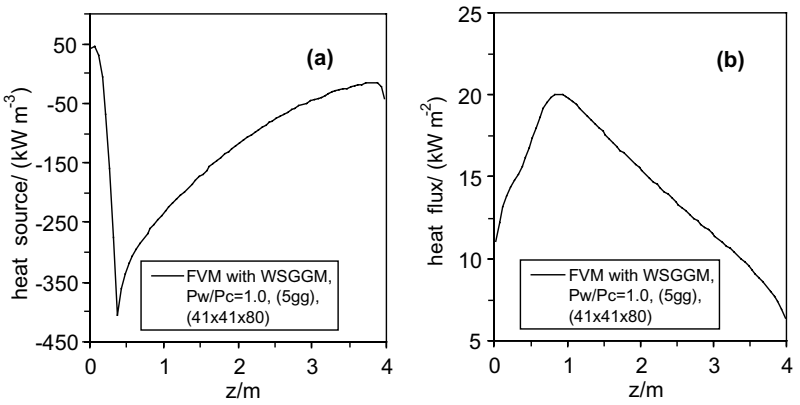

Fig. 4. Predictions of radiative heat source and incident heat flux for test case 4: (a) radiative heat source along the centerline (1 m, 1 m, z); (b) incident heat flux along (2 m, 1 m, z).

Fig. 4(a) and (b) shows the predictions of the radiative heat source along centerline (1 m, 1 m, z) and of the incident heat flux along (2 m, 1 m, z) respectively for test case 4. The five gray gases model (5gg) was applied. The uniform rectangular grid $41\times41\times80$ is used. The angular discretization, polar $\times$ azimuthal, is 4×20.

The same predictions for test case 4 as in Fig. 4(a) and (b) are reported in Tables 1 and 2. These are given for the sake of comparisons with predictions to be provided by the others.

6. Conclusions

1. A new mathematical model and computer code for non-gray-gases radiation in 3-D rectangular enclosures based on coupling of FVM with WSGGM is developed. The physical and mathematical concepts of the model are thoroughly presented. The Smith et al.'s WSGG model was incorporated, but any other gas radiative properties model can be introduced as well in the same way. The series of predictions were performed for pure water vapor and for the mixtures of water vapor, carbon dioxide and nitrogen for uniform and non-uniform temperature fields. The predictions, calculated with 4gg and 5gg, were compared against the rare results found in literature. The variation of spatial rectangular grid and of angular discretization in polar and azimuthal directions was performed and their influence on accuracy was analyzed.
2. The differences between model predictions and benchmark results arise, inter alia, because the surface temperatures, or so-called irradiation temperatures T_s in all calculation cases are set at 300 K, while the WSGG model used here [19] is designed and is good for region $600 < T_s < 2400$ K. Irradiation temperature T_s plays important role for the evaluation of total gas absorptivity, or in this model for the evaluation of absorptivity weighting factors. This is discussed in the last paragraph of Section 2.5.
3. Only benchmark results for 3-D non-gray gas radiation found in literature [30] is for $T_s = 300$ K. Once the benchmark values for the region of irradiation temperatures $600 < T_s < 2400$ K are available, the predictions by this model can be performed within that region. Much better agreement between predictions and benchmark can be expected then.
4. New mathematical model and code are very reliable and the accuracy of the predictions depends very much on the accuracy of the gas radiative properties model that is incorporated in.
5. The predictions obtained by this mathematical model have the same accuracy as the results calculated previously by DOM with WSGGM if the radiative properties model for 4gg was used. By increasing the number of gray gases from four to five, within WSGGM, the accuracy of the predictions of radiative heat source is significantly improved and these predictions can be used in engineering calculations.
6. Since 5gg WSGGM showed very good accuracy, a concept of economical and accurate non-gray-gases radiation modeling can be proposed herewith. It consists of (i) development of the 5gg WSGGM for the non-gray-gas under consideration and (ii) coupling of that 5gg model with FVM according to the new methodology developed in this paper.
7. FVM is widely used for solving transport equations within CFD codes nowadays. By solving RTE for non-gray gases with FVM and avoiding computationally very expensive spectral lines and bands models by replacing them with WSGGM, makes this radiation model and code compatible and convenient for coupling with CFD codes.

Table 1
Distribution of radiative source along the centerline and of heat flux along (2 m, 1 m, z) for case 4, first part for z values from $z = 0.025$ to 1.975 m

z (m)	Radiative heat source (kW m^{-3})	Incident heat flux (kW m^{-2})
0.025	43.523	11.062
0.075	45.198	12.226
0.125	30.841	13.117
0.175	−6.350	13.818
0.225	−70.272	14.364
0.275	−160.771	14.800
0.325	−274.054	15.192
0.375	−405.615	15.623
0.425	−360.809	16.131
0.475	−335.333	16.733
0.525	−318.470	17.385
0.575	−305.611	18.034
0.625	−294.830	18.631
0.675	−285.239	19.139
0.725	−276.389	19.534
0.775	−268.038	19.811
0.825	−260.049	19.974
0.875	−252.345	20.035
0.925	−244.877	20.012
0.975	−237.617	19.921
1.025	−230.544	19.779
1.075	−223.642	19.601
1.125	−216.900	19.398
1.175	−210.310	19.179
1.225	−203.863	18.951
1.275	−197.553	18.718
1.325	−191.372	18.483
1.375	−185.316	18.248
1.425	−179.381	18.014
1.475	−173.561	17.782
1.525	−167.854	17.552
1.575	−162.259	17.324
1.625	−156.769	17.098
1.675	−151.387	16.875
1.725	−146.109	16.653
1.775	−140.933	16.432
1.825	−135.858	16.214
1.875	−130.886	15.997
1.925	−126.013	15.781
1.975	−121.241	15.566

Table 2
Distribution of radiative source along the centerline and of heat flux along (2 m, 1 m, z) for case 4, second part for z values from $z = 2.025$ to 3.975 m

z (m)	Radiative heat source (kW m^{-3})	Incident heat flux (kW m^{-2})
2.025	−116.568	15.352
2.075	−111.996	15.140
2.125	−107.523	14.928
2.175	−103.150	14.718
2.225	−98.877	14.509
2.275	−94.703	14.301
2.325	−90.629	14.094
2.375	−86.655	13.889
2.425	−82.780	13.685
2.475	−79.005	13.483
2.525	−75.330	13.282
2.575	−71.755	13.083
2.625	−68.279	12.885
2.675	−64.901	12.689
2.725	−61.622	12.495
2.775	−58.441	12.303
2.825	−55.357	12.112
2.875	−52.371	11.923
2.925	−49.482	11.735
2.975	−46.688	11.548
3.025	−43.989	11.362
3.075	−41.386	11.175
3.125	−38.876	10.987
3.175	−36.460	10.797
3.225	−34.138	10.605
3.275	−31.911	10.410
3.325	−29.780	10.209
3.375	−27.748	10.003
3.425	−25.819	9.790
3.475	−24.000	9.569
3.525	−22.298	9.338
3.575	−20.726	9.098
3.625	−19.299	8.847
3.675	−18.041	8.583
3.725	−16.999	8.305
3.775	−16.272	8.011
3.825	−16.113	7.697
3.875	−17.222	7.352
3.925	−21.883	6.944
3.975	−40.780	6.369

Acknowledgements

The financial support for this work was provided by the US Department of Energy (DOE), National Energy Technology Laboratory (NETL), Morgantown, WV, within the Radiation Project for years 2001 and 2002. The work was carried out at Institute for Complex Engineered Systems (ICES), Carnegie Mellon University, Pittsburgh, PA. The author gratefully acknowledges the assistance of Dr. Thomas O'Brien, Research Scientist from DOE, NETL, Morgantown, WV and of the Director of ICES, Cristina H. Amon, Raymond R. Lane, Distinguished Professor of Mechanical Engineering, Carnegie Mellon University, who kindly made author's prediction data available. A part of the support related to the purchasing of an airplane ticket Belgrade–Pittsburgh, of a last generation Dell computer and for final paper writing was provided by Ministry of Science, Technology and Development, Republic of Serbia, within Project No. 1891. Without all these financial supports the paper would not be finished and author would like to express his deep gratitude to all of them.

References

[1] M.F. Modest, H. Zhang, The full-spectrum correlated-*k* distribution and its relationship to the weighted-sum-of-gray-gas method, in: Proceedings of the 2000 IMECE, vol. HTD-366-1, ASME, Orlando, FL, 2000, pp. 75–84.

[2] H.C. Hottel, A.F. Sarofim, Radiative Transfer, McGraw-Hill, New York, 1967.

[3] N. Lallemant, A. Sayre, R. Weber, Evaluation of emissivity correlations for H_2O–CO_2–N_2/air mixture and coupling with solution methods of the radiative transfer equation, Progr. Energy Combust. Sci. 22 (1966) 543–574.

[4] M.N. Ozisik, Radiative Transfer, A Wiley-Interscience Publication, New York, 1973.

[5] R.M. Goody, R. West, L. Chen, D. Chrisp, The correlate-*k* method for radiation calculations in non-homogenous atmospheres, J. Quant. Spectrosc. Radiat. Transfer 42 (1989) 539–550.

[6] A.A. Lacis, V. Oinas, A description of the correlated *k*-distribution method for modeling non-gray gaseous absorption, thermal emission, and multiple scattering in vertically inhomogeneous atmospheres, J. Geophys. Res. 96 (1991) 9027–9063.

[7] L.S. Rothman, R.R. Gamache, R.H. Tipping, C.P. Rinsland, M.A.H. Smith, D. Chris Benner, V. Malathy Devi, J.M. Flaud, C. Camy-Peyret, A. Perrin, A. Goldman, S.T. Masie, L.R. Brown, The HITRAN molecular database: editions of 1991 and 1992, J. Quant. Spectrosc. Radiat. Transfer 48 (5/6) (1992) 469–507.

[8] M.K. Denison, B.W. Web, A spectral line-based weighted-sum-of-gray-gases model for arbitrary RTE solvers, ASME J. Heat Transfer 115 (1993) 1004–1012.

[9] F. Liu, G.J. Smallwood, O.L. Gulder, Application of the statistical narrow band correlated-*k* method to non-gray gas radiation in CO_2–H_2O mixtures: approximate treatments of overlapping bands, J. Quant. Spectrosc. Radiat. Transfer 68 (2001) 401–417.

[10] F. Liu, G.J. Smallwood, O.L. Gulder, Application of the statistical narrow band correlated-*k* method to non-gray gas radiation in CO_2–H_2O mixtures—effects of the quadrature scheme, Int. J. Heat Mass Transfer 43 (2000) 3119–3135.

[11] O. Marin, R.O. Buckius, Wideband correlated-*k* method applied to absorbing, emitting and scattering media, J. Thermophys. Heat Transfer 10 (1996) 364–371.

[12] F. Liu, G.J. Smallwood, O.L. Gulder, Band lumping strategy for radiation heat transfer using a narrow band model, J. Thermophys. Heat Transfer 14 (2000) 278–281.

[13] M.K. Denison, B.W. Web, The spectral line-based weighted sum of gray gases model in nonisothermal and nonhomogenous media, ASME J. Heat Transfer 117 (1995) 359–363.

[14] L. Pierrot, Ph. Riviere, A. Soufiany, J. Taine, A-fictious-gas-based absorption distribution function global model for radiative transfer in hot gases, J. Quant. Spectrosc. Radiat. Transfer 62 (1999) 609–624.

[15] L. Pierrot, A. Soufiany, J. Taine, Accuracy of narrow-band and global models in H_2O, CO_2 and H_2O–CO_2 mixtures at high temperatures, J. Quant. Spectrosc. Radiat. Transfer 62 (1999) 523–548.

[16] M.F. Modest, The weighted-sum-of-gray-gases model for arbitrary solution methods in radiative transfer, ASME J. Heat Transfer 113 (3) (1991) 650–656.

[17] F.R. Steward, Y.S. Kocaefe, in: U. Grigull, E. Hahne, K. Stephan, J. Straub (Eds.), Proceedings of the 7th International Heat Transfer Conference, vol. 2, Munchen, 1982, pp. 553–558.

[18] F.R. Steward, Y.S. Kocaefe, in: C.L. Tien, C.V. Carey, Ferel (Eds.), Proceedings of the 8th International Heat Transfer Conference, Hemisphere Publishing Corporation, New York, 1986, pp. 735–740.

[19] T.F. Smith, Z.F. Shen, J.N. Fridman, Evaluation of coefficients for the weighted sum of gray gases model, ASME J. Heat Transfer 104 (1982) 602–608.

[20] S. Maruyama, Z. Guo, Radiative heat transfer in arbitrary configurations with non-gray absorbing, emitting and anisotropic scattering media, J. Heat Transfer 121 (1999) 722–726.

[21] A. Soufiani, E. Djavan, A comparison between weighted-sum-of-gray-gases and statistical narrow-band radiation models for combustion applications, Combust. Flame 97 (1994) 240–250.

[22] J.G. Marakis, E. Kakaras, X. Kakatsios, N. Papageorgiou, Application of the direct numerical integration method in a cylindrical geometry containing non-gray pressurized gases, in: Proceedings Eurotherm # 56, Heat Transfer in Radiating and Combusting Systems-3, 1–3 April 1988, Delphy, Greece, pp. 263–274.

[23] L. Zhang, A. Soufiani, J. Taine, A spectral correlated and non-correlated radiative transfer in a finite axisymmetric system containing an absorbing and emitting real gas–particle mixture, Int. J. Heat Mass Transfer 31 (1988) 2261–2272.

[24] P.S. Cumber, M. Fairweather, H.S. Ledin, Application of wide band radiation models to non-homogenous combustion systems, Int. J. Heat Mass Transfer 41 (1988) 1573–1584.

[25] M.K. Denison, A spectral line-based weighted-sum-of-gray-gases model for arbitrary RTE solvers, Ph.D. Thesis, Mechanical Engineering Department, Brigham Young University, Provo, UT, 1994.

[26] V. Goutiere, F. Liu, A. Charette, An assessment of real-gas modeling in 2D enclosures, J. Quant. Spectrosc. Radiat. Transfer 121 (1999) 200–203.

[27] D.N. Trivic, Mathematical modeling of three-dimensional turbulent flow with combustion and radiation, Ph.D. Thesis, Department of Chemical Engineering, University of New Brunswick, Fredericton, NB, Canada, 1987.

[28] F.R. Steward, D.N. Trivic, An assessment of particle radiation in a pulverized-coal-fired boiler, J. Instit. Energy 452 (1989) 138–146.

[29] P.J. Coelho, Numerical simulation of radiative heat transfer from non-gray gases in three-dimensional enclosures, J. Quant. Spectrosc. Radiat. Transfer 74 (2002) 307–328.

[30] F. Liu, Numerical solutions of three-dimensional non-gray gas radiative transfer using the statistical narrow-band model, Trans. ASME 121 (1999) 200–203.

[31] A. Soufiani, J. Taine, High temperature gas radiative property parameters of statistical narrow band model for H_2O, CO_2 and CO and correlated-*k* (CK) model for H_2O and CO_2, Int. J. Heat Mass Transfer 40 (1997) 987–991.

[32] R. Siegel, J.R. Howell, Thermal Radiation Heat Transfer, Hemisphere Publishing Corporation, New York, 1993.
[33] J.C. Chai, Finite Volume method for radiation heat transfer, Ph.D. Dissertation, University of Minnesota, Minneapolis, MN, 1994.
[34] J.C. Chai, H.S. Lee, S.V. Patankar, Finite volume method for radiation heat transfer, J. Thermophys. Heat Transfer 8 (3) (1994) 419–425.
[35] J.C. Chai, S.V. Patankar, Finite Volume Method for Radiation Heat Transfer, in: Minkowitz, Sparrow (Eds.), Advances in Numerical Heat Transfer, vol. 2, Taylor & Francis, London, 2000.
[36] G.D. Raithby, E.H. Chui, A finite-volume method for predicting a radiant heat transfer in enclosures with participating media, J. Heat Transfer 112 (2) (1990) 415–423.
[37] H.C. Hottel, A.F. Sarofim, The effects of gas flow patterns on radiative transfer in cylindrical enclosures, Int. J. Heat Mass Transfer 8 (1965) 1153–1169.
[38] M.F. Modest, Radiative Heat Transfer, McGraw-Hill, New York, 1993.